G-2-3

Extended Abstracts of the 2013 International Conference on Solid State Devices and Materials, Fukuoka, 2013, pp826-827

Fabrication and Evaluation of Differential Si Ring Optical Resonator for Biosensors

Tomoya Taniguchi[1], Yoshiteru Amemiya[1], Takeshi Ikeda[3,1], Akio Kuroda[3,1], and Shin Yokoyama[1,2]

[1]Res. Inst. for Nanodevice and Bio Systems, Hiroshima Univ. [2]Dept of Semiconductor Electronics and Integration
[3]Dept of Molecular Biotechnology, Graduate School of Advanced Sciences of Matter (AdSM), Hiroshima Univ.
1-4-2 Kagamiyama, Higashihiroshima, Hiroshima 739-8527, Japan
Phone: +81-82-424-6265, Fax: +81-82-424-3499, E-mail: taniguchi-tomoya@hiroshima-u.ac.jp

1. Introduction

We are studying biosensors detectable plural kinds of reactions rapidly without labeling [1-3]. The schematic structure of the target integrated biosensor is shown in Fig. 1. The Si ring biosensor is compact and suitable for the integration. However, the sensitivity for biosensing is not sufficiently high and the improvement has been done for example by using slot waveguide [2,3]. Figure 2 shows the fabricated ring biosensor with slot waveguide. An example of biosensing using Si slot ring biosensor is shown in Fig. 3 for the prostate specific antigen (PSA) [3]. The sensitivity is 10^{-8} g/ml, while the practically required sensitivity is 10^{-9} g/ml. Hence, further one order of magnitude of improvement is required, which is expected by using the differential sensing.

2. Operation principle of biosensor

Structure of the differential biosensor is shown in Fig. 4. There are two rings for reference and sensing. One of the two outputs is connected to 180° phase shifter, and merged again. The measurement principles for the direct and differential sensing methods are compared in Fig. 5. Figure 5(a) shows the direct sensing method, where the wavelength of the input laser is fixed at the steepest point of the resonance curve ($\lambda_{res} \pm w\sqrt{3}/6$, where λ_{res} and w are resonance wavelength and FWHM, respectively). The minimum detectable concentration of the sensing substance, n, is given by,

$$n = \frac{4\sqrt{3}N_{oise}\lambda_{res}}{3KQ} = 2.31 \times \frac{N_{oise}\lambda_{res}}{KQ}, \quad (1)$$

where, N_{oise} is noise signal intensity, λ_{res} is the resonance wavelength, K is the equilibrium constant for the Langmuir adsorption equation, and Q is the quality factor of the resonator [4]. The eq. (1) is derived assuming the resonance curve as Lorentzian and the Langmuir adsorption. In order to increase the sensitivity, the quality factor Q of the resonator must be high. However, since the FWHM of the input laser is finite (0.045 nm in this study), the output signal is reduced when Q becomes high because both signal increase and decrease portions exist within the FWHM and cancelled. On the other hand for the differential sensing (see Fig. 5 (b)) temperature fluctuation and stray light or any common mode noises are cancelled. And also wide FWHM input laser is available.

3. Performance of phase shifter

The 180° phase shifter is important in the differential detection. We have designed the Mach-Zehnder interferometer type phase shifter because it is simple structure and easy to obtain a high output intensity. The fabrication process is conventional electron beam lithography and dry etching reported in Ref. [1]. The fabricated phase shifter is shown in Fig. 6(a) where the amount of the phase shift is controlled by the displacement of the output waveguide position Δx. Simultaneously the differential Si ring biosensors were fabricated on the same wafer (Fig. 6(b)). The characteristics of the phase shifter in water and air are shown in Fig. 7. Both of the curves well fit to the theoretical cosine curve, $\cos^2\theta/2$, where θ is the phase shift. In the water (blue curve), the optical output intensity takes a minimum at the shorter physical path difference because the refractive index of the water (1.33) is larger than that of the air (1).

4. Measurement of resonance wavelength shift

The shift of the resonance wavelength was measured after silicone grease (n=1.5) was attached on the each ring. The result is shown in Fig. 8. The upper graph is for the initial condition (no grease). The center graph shows that after putting silicone grease on the reference ring. A remarkable shift of the resonance wavelength is observed. Next, the silicone grease was attached to the sensing ring too. As a result another resonance peak-shift of the sensing ring is clearly observed. The discrepancy in the amount of the resonance peak-shifts for these rings may be due to the difference in the area covered with the silicone grease.

5. Conclusions

The differential Si-ring biosensor was fabricated. The performance of the 180° phase shifter was confirmed. The resonance wavelength shift of each ring in the differential sensor was confirmed by putting silicone grease.

Acknowledgement

This study was partially supported by a Grant-in-Aid for Scientific Research (B) (246360136, 2012) from the Ministry of Education, Culture, Sports, Science and Technology of Japan.

References

[1] M. Fukuyama *et al*., Jpn. J. App. Phys. **50** (2011) 04DL07.
[2] M. Fukuyama *et al*., Jpn. J. App. Phys. **50** (2011) 04DL11.
[3] A. Hirowatari *et al*., Proc. SPIE Photonics Europe 2012, **8431** (2012) 63.
[4] M. Fukuyama, Doctor Thesis, Graduate School of AdSM, Hiroshima Univ. 2011, p. 18.

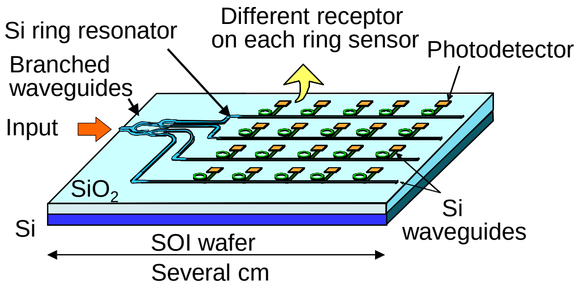

Fig. 1. Target integrated biosensor which provides simultaneous sensing of multi bio species. Ring resonator sensors are suitable because of their compactness.

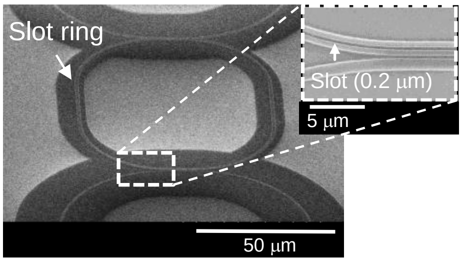

Fig. 2. Scanning electron microscope (SEM) image of the slot ring biosensor fabricated in our lab. The slot (width of 0.2 μm) is very effective to enhance the sensitivity. However, the further improvement of sensitivity and temperature stability are required for practical use.

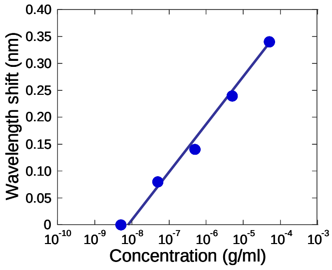

Fig. 3. Resonance wavelength shift of the Si ring biosensor for prostate specific antigen (PSA). The practically required sensing concentration is ~10^{-9} g/ml. Further one order of magnitude sensitivity-improvement will be possible by slot ring and differential sensing.

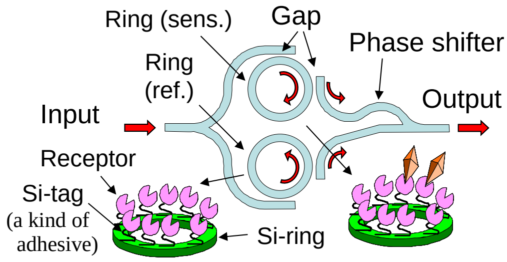

Fig. 4. Proposed differential type ring resonator sensor, which has special features such as high sensitivity due to the common-mode-noise cancellation and high temperature stability by the same temperature dependence of the reference and sensing rings.

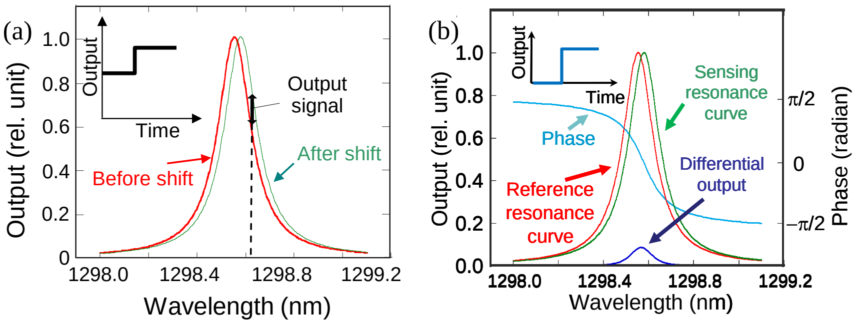

Fig. 5. Principle of biosensing for (a) previous direct sensing and (b) differential sensing. For direct sensing the temperature fluctuation and stray light cause the serious problems. On the other hand for the differential sensing both of these noise sources are cancelled. The structure is simple: one of the output of two rings are connected to 180° phase shifter, and merged again as shown in Fig. 4.

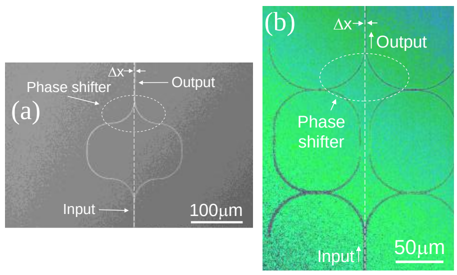

Fig. 6. (a) shows an SEM image of the phase shifter with MZI and (b) shows the differential Si ring optical resonator. The optical path difference is generated by shifting the axis of the input and output ports.

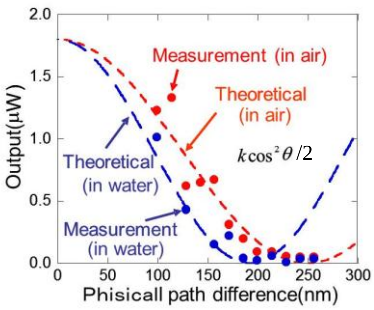

Fig. 7. Characteristics of the phase shifter. In the water (blue), the optical output intensity takes minimum at the shorter physical path difference because the refractive index of the water (1.33) is larger than that of the air (1).

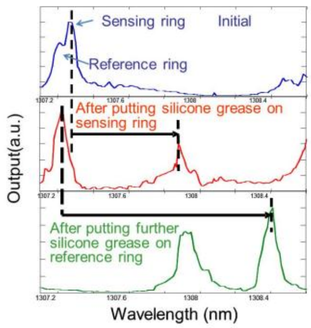

Fig. 8. Shifts of the resonance peaks of the reference and sensing Si rings by putting silicone grease on each ring. The shift of the resonance peak of each ring is separately observed.